which yields

$$\frac{1}{T(\tau_0)}\left(\frac{d}{d\tau}T(\tau)\right)_{\tau=\tau_0} = \tan(\tau_0 - \phi). \tag{58}$$

The contour of integration, $C$, is then chosen such that the path goes through the saddle point, $\tau_0$, and that the imaginary part of $u$ is constant. Following the method of steepest descent, the solution for (55) is therefore

$$I^i = \frac{S^i(\tau_0)}{2n(\tau_0)} \frac{e^{-Ru(\tau_0)}}{R(\sin\phi)^{1/2}} \tag{59}$$

where

$$n(\tau_0) = \left\{2T\sin\tau\left[\left(\frac{dT}{d\tau} - T\right)\cos(\tau - \phi) - 2\frac{dT}{d\tau}\sin(\tau - \phi)\right]\right\}^{1/2}_{\tau=\tau_0}. \tag{60}$$

The electric field intensity $\boldsymbol{E}$ in infinite domain may, therefore, be obtained from

$$\boldsymbol{E} = \sum_i \int_{v_0} \left[(L^i)(L_0^{*i}) \frac{S^i(\tau_0)}{2n(\tau_0)} \frac{e^{-jRu(\tau_0)}}{R(\sin\phi)^{1/2}}\right] \cdot \boldsymbol{I}_s dv_0 \tag{61}$$

providing that all parameters, including the differential operators, are properly transformed to the correct observer and source coordinates in the spherical coordinate system.

The Green's dyadic as shown in (61) is in a form different from those obtained either by Lee and Papas or by Compton and Tai. Nevertheless, the results should be equivalent.

### Acknowledgment

The author wishes to express his appreciation to S. E. Longo of Tulane University, Department of Electrical Engineering, for reading this manuscript, and to Mrs. Jan E. Borhaug who patiently typed the many revisions to this manuscript.

# Coupler-Type Bend for Pillbox Antennas

VINCENT MAZZOLA, MEMBER, IEEE, AND JOEL E. BECKER, SENIOR MEMBER, IEEE

*Abstract*—**A new type of 180° $H$-plane bend has been developed for use in double-layer pillbox antennas. This bend, called a coupler-type bend, permits complete coupling between two pillbox layers with a minimum of reflection, cross-polarization, and defocusing. It can be used with short focus antennas where large feed angles are involved. The coupler-type bend utilizes a metal plate between the pillbox layers; the plate contains a pattern of holes which achieves the desired coupling.**

**Analytical and experimental programs have been implemented to determine the optimum hole size and distribution. Simulation techniques in rectangular waveguide were employed for convenience in measurements. The bend design was measured to have a reflection less than 2 dB SWR over a ten percent frequency band; this is computed to contribute less than 0.2 dB SWR to the reflection seen by the feed-horn of a double-layer pillbox. The bend introduces less than −22 dB of cross-polarization in the antenna radiation. Measurements of a pillbox model incorporating the bend design have verified the predicted performance of the coupler-type bend.**

## I. Introduction

ONE OF THE common antennas for generating a fan beam is the pillbox or "cheese" antenna [1], [2]. For the single-layer pillbox antenna, the feed is usually located in the radiating aperture, producing several undesirable effects. First, a portion of the wave in the aperture is received by the feed and appears as a reflection. Second, this blocking causes a hole in the aperture excitation giving rise to degradation of the pattern in the form of higher sidelobes.

In order to eliminate these effects, double-layer pillboxes have been developed [2]. In the double-layer arrangement, the feed is located in one layer with the second layer containing the aperture. In such designs, the principal problem is to transfer the wave efficiently from one layer to the other. In the past, this has been accomplished with a bend consisting of a large slot in the common wall between the layers, bordering along the entire length of the parabolic reflector. In general, this configuration has been successful only over a narrow bend of frequencies and for long focal-length pillboxes, in which the bend is required to operate only over a narrow range of angles. In addition, there is frequently the problem of appreciable antenna response to cross-polarization. All of these defects can be traced to the performance of the coupling device.

A new double-layer pillbox has been developed at Wheeler Laboratories which operates over a substantially larger band of frequencies and with a larger feed angle (shorter focal length) than possible in the past. Also, cross-polarization is suppressed to a tolerable level. This performance has been achieved by an improved coupling device between the layers; the device is referred to as a coupler-type bend [3].

Manuscript received April 3, 1967. This work was performed on a subcontract from Bell Telephone Laboratories, Inc. The prime contract was between the Western Electric Company and the U. S. Army.

The authors are with Wheeler Laboratories, Inc., Smithtown, N. Y. 11787

The bend has been designed to operate in an $E$-plane pillbox (electric field parallel to the flat walls of the pillbox); it consists of an array of holes in the common wall between layers located along the entire length of the parabolic wall. The hole diameter was optimized to provide wideband performance in a compact design. This type of bend has a high power capacity which is required for many radar applications.

## II. Symbols

The symbols used in this paper are collected here for reference.

$d$ = coupling hole diameter
$a$ = wall separation in the pillbox
$L$ = length of coupling region, normal to pillbox reflecting surface
$L_0$ = length of coupling region at normal incidence
$\lambda$ = wavelength in free space
$\lambda_g$ = guide wavelength
$\lambda_{ca}$ = cutoff wavelength for the antisymmetric mode $= 2a$
$\lambda_{ga}$ = guide wavelength for the antisymmetric mode $= \lambda/\sqrt{1-(\lambda/\lambda_{ca})^2}$
$\lambda_{gs}$ = guide wavelength for the symmetric mode
$\lambda_r$ = coupling-hole resonant wavelength
$f_0$ = midband frequency
$\theta$ = angle of incidence at the coupling region
$\theta'$ = angle of propagation in the coupling region for the symmetric mode
$c$ = voltage coupling coefficient for single hole
$C$ = voltage coupling coefficient for array of holes
$n$ = number of coupling holes
$N$ = number of coupling holes for complete coupling
dB SWR = standing-wave ratio expressed in dB
dB $R$ = reflection coefficient expressed in dB.

## III. Description

Shown in Fig. 1 is the type of double-layer pillbox for which the coupler-type bend was designed. It is shown with an aperture to focal-length ratio of four. Illumination of the pillbox is achieved with a waveguide horn. The horn is located in the lower (feed) layer and the aperture in the upper layer. Metal walls (feed walls) are attached to both sides of the horn and serve to close off the lower layer. The separation between the plates of the pillbox is maintained by vertical metal support posts which are perpendicular to the $E$ field and therefore have little electrical effect. The coupler-type bend is the region which contains the triangular array of holes of the common wall between layers adjacent to the parabolic wall.

The operation of the bend can be explained by recognizing that propagation in the pillbox is in accordance with the principles of geometric optics. That is, energy radiated by the feed follows ray paths having a circular wavefront. When the rays enter the coupling region from the feed layer, energy begins coupling to the aperture layer. At the parabolic-wall reflecting surface, one-half the power has been transferred

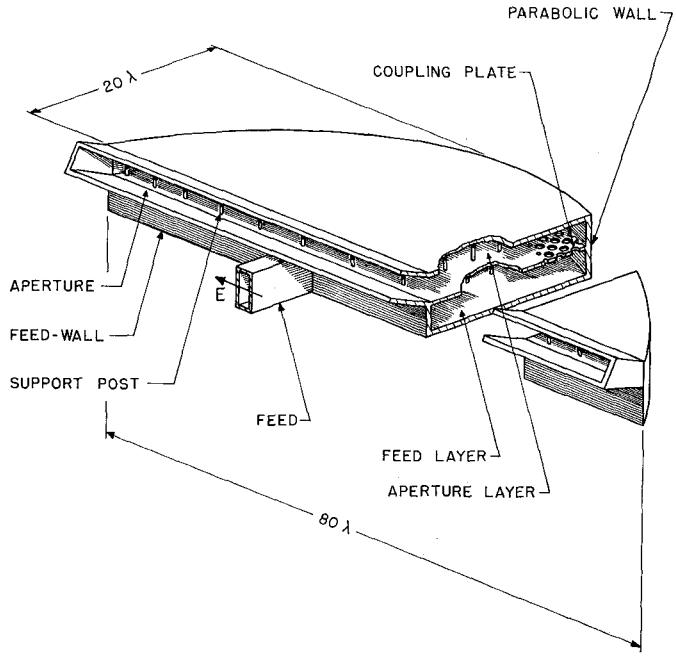


Fig. 1. Double-layer pillbox employing a coupler-type bend.

The reflecting surface redirects the rays so they are parallel (a plane wavefront). The coupling of these reflected rays into the aperture layer is complete at the edge of the coupling region.

The holes are circular to provide the same coupling for all directions of propagation; they are arranged in a triangular pattern in order to obtain good directivity. The number of holes together with the diameter of the leading hole is specified for each location in the pillbox thus providing complete coupling along the entire bend.

## IV. Design Approach

The design of the coupling region incorporates three parameters: hole diameter, length of the coupling region, and separation between the pillbox plates. At normal incidence (where rays enter normal to the coupling region), hole diameter and plate separation are utilized to obtain a design. The procedure is to select a combination of these dimensions which yields the shortest coupling length along with a flat coupling characteristic with frequency. At oblique incidence (where rays are incident at an angle to the coupling region), the hole diameter and wall separation are identical to that for normal incidence. In order to achieve complete coupling, the length of the coupling region is made smaller as the angle of incidence of the rays increases.

### A. Normal Incidence

For a small region at normal incidence, the bend can be considered to be equivalent to a directional coupler with full coupling (0 dB). In this region of the bend, one can approximate the parabolic wall by a plane reflector which can then be replaced by the image of the coupling region. This equivalence is illustrated in Fig. 2(a). In the imaged version, the output wave emerges in the pillbox layer diagonally opposite

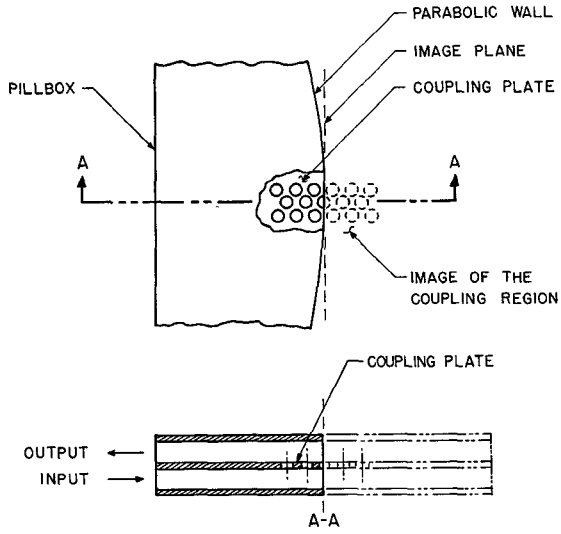


(a) Image of the bend.

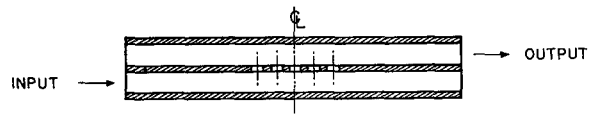


(b) Directional coupler equivalent to the bend.

Fig. 2. Coupling in the bend at normal incidence.

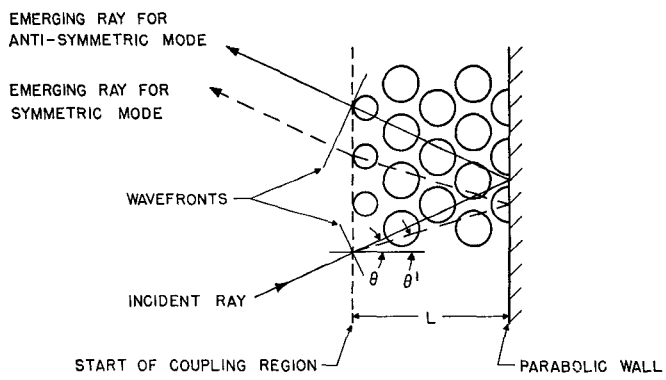


(a) Ray paths for symmetric and antisymmetric mode.

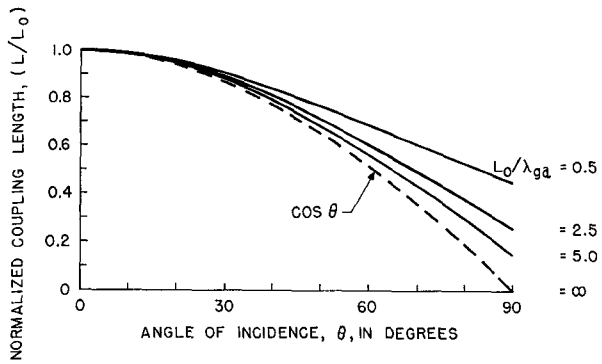


(b) Variation of coupling length with angle.

Fig. 3. Coupling in the bend at oblique incidence.

to the input layer; the result can be considered to be a directional coupler with an infinite $E$-plane dimension. This coupler is shown in Fig. 2(b). This infinite $E$-plane structure has the same properties as a finite structure with metal walls perpendicular to the original parabolic reflector and arranged so that they image the array of holes. The resulting equivalent structure is a conventional directional coupler. The equivalence between the bend and directional coupler is useful in the design of the bend because it separates the reflection arising from the discontinuity at the input to the coupling region from the reflection caused by incomplete transfer of the power in the coupling region. The normal-incidence reflection seen in the input to the pillbox bend is found to be identical to the vector sum of the input reflection of the coupler and the component of the wave which fails to be coupled. Thus, if the reflection coefficient of the equivalent coupler and the uncoupled signal were each $-26$ dB $R$, the maximum reflection of the resulting pillbox bend design would be $-20$ dB $R$ (1.7 dB SWR). For the bend to be matched, the equivalent coupler must be designed for 0 dB coupling and perfect match and directivity.

### *B. Oblique Incidence*

The design variable for oblique incidence is the length of the coupling region, which must be adjusted to provide full coupling at all angles of incidence. The change in length is necessary because the ray path length through a fixed length of coupling region increases with increasing angle of incidence.

Figure 3 shows a sample of the coupling region for obliquely incident rays. The transfer of power in the coupling region results from the dispersion between a symmetric and antisymmetric mode which propagate in that region. This viewpoint has previously been used for the analysis of directional couplers [4], [5]. Figure 3(a) illustrates the ray paths for these two modes. For full transfer, the relative phase shift between the modes must be 180 degrees for a complete path (forward and reflected) through the coupling region. Analysis of this condition yields the following formula for the required coupling length in terms of the angle of incidence and the guide wavelengths of the two modes:

$$\lambda_{ga}/4L = \sqrt{(\lambda_{ga}/\lambda_{gs})^2 - \sin^2\theta} - \cos\theta. \tag{1}$$

At normal incidence ($\theta = 0°$), this equation reduces to

$$1 + \lambda_{ga}/4L_0 = \lambda_{ga}/\lambda_{gs}. \tag{2}$$

Substituting for $\lambda_{ga}/\lambda_{gs}$, (1) becomes:

$$\lambda_{ga}/4L = \sqrt{\left[1 + \frac{\lambda_{ga}}{4L_0}\right]^2 - \sin^2\theta} - \cos\theta. \tag{3}$$

The antisymmetric mode cutoff wavelength $\lambda_{ca}$ is, in general, a function of wall thickness (and hole size) as well as guide width. If the wall is assumed to be negligibly thin, the

cutoff wavelength $\lambda_{ca}$ is $2a$. Thus, the antisymmetric mode guide wavelength is known in terms of the plate separation, $a$, by the relation $\lambda_{ga}=\lambda/\sqrt{1-(\lambda/2a)^2}$. Utilizing (3), the quantity $L/L_0$ is plotted in Fig. 3(b) as a function of the angle $\theta$ with the quantity $L_0/\lambda_{ga}$ as a parameter.

### C. Selection of Hole Diameter

The design of the coupling region at normal incidence is obtained by using hole diameter and plate separation as variables. These variables are optimized in the directional coupler model to yield a matched coupler having zero dB coupling over the frequency band of interest. For the directional coupler model, the plate separation in the pillbox, $a$, is equivalent to the $H$-plane dimension of the coupler waveguide. The effective spacing of the holes in the sidewall is chosen to be a quarter-guide-wavelength for good directivity. In order to achieve a short coupling length, large closely-packed holes are used. For large holes in the sidewall of a waveguide, a coupling formula is not available in the literature. However, Cohn has given results for circular irises in the transverse plane which can be applied here [6]. This approach results in an approximate formula giving the coupling trend for a single hole as

$$c \propto \frac{\lambda_{ga}}{1-(\lambda_r/\lambda)^2} = \frac{\lambda}{\{1-(\lambda_r/\lambda)^2\}[1-(\lambda/2a)^2]^{1/2}}. \quad (4)$$

The resonant wavelength of the hole, $\lambda_r$, is approximately the cutoff wavelength of the lowest-order TE mode in the circular cross section of the hole; this is $1.706d$.

From (4) it is found that there is a value of wavelength for which the coupling slope is zero. This wavelength is found by differentiating coupling with respect to wavelength and setting the expression equal to zero. The result is

$$3/\lambda^2 = 1/\lambda_r^2 + 2/(2a)^2. \quad (5)$$

Substituting $\lambda_r = 1.706d$, (5) is rewritten as

$$8.73 = (\lambda/d)^2 + 5.82(\lambda/2a)^2. \quad (6)$$

Equation (6) is shown plotted as a dashed line in Fig. 4, on the coordinates $(\lambda/2a)^2$ and $(\lambda/d)^2$ which give a linear representation; this line is labeled in the figure as the line of zero-slope coupling. Thus, in order to obtain a flat coupling characteristic with frequency, values of $a$ and $d$ must be chosen which lie along this line.

In addition to the requirement of zero-slope coupling, good directivity must be maintained. For the triangular arrangement of holes shown in Fig. 4, the effective spacing between the holes in the direction of propagation is chosen to be $\lambda_{ga}/4$. This condition can be written as

$$d \cos \alpha = \lambda_{ga}/4. \quad (7)$$

The angle $\alpha$ specifies a particular triangular arrangement and is defined in Fig. 4. Substituting for $\lambda_{ga}$, the following expression is obtained

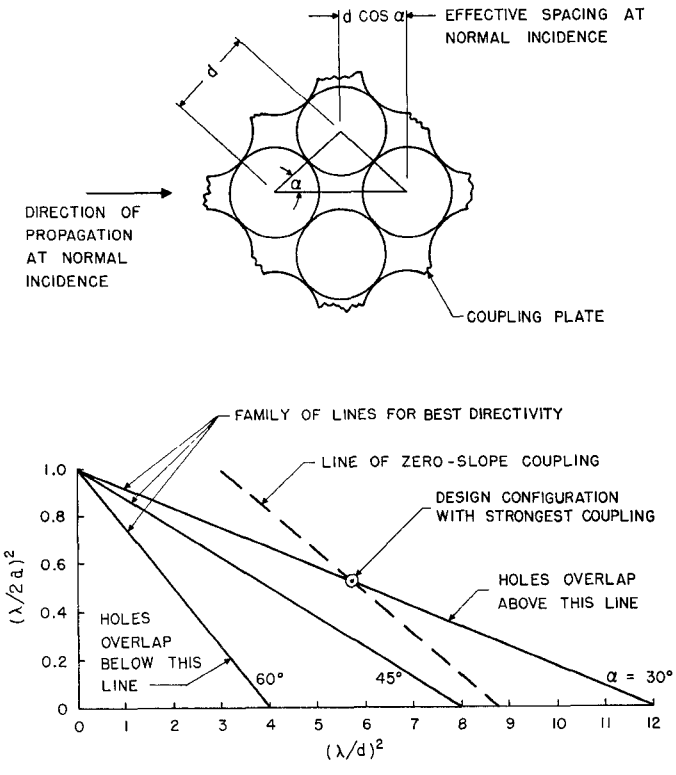


Fig. 4. Array dimensions for directivity and zero-slope coupling.

$$16 \cos^2 \alpha = (\lambda/d)^2 + 16(\lambda/2a)^2 \cos^2 \alpha. \quad (8)$$

Equation (8) is plotted as the solid lines in Fig. 4. This equation, expressing the condition for directivity, yields a family of straight lines with the angle $\alpha$ as the parameter. The region in which this equation is valid is described in Fig. 4 as the region between the lines labeled $\alpha=30°$ and $\alpha=60°$. For values of the angle $\alpha$ less than 30°, the vertical pair of the holes shown in Fig. 4 would overlap; for $\alpha$ greater than 60°, the horizontal pair of holes would overlap. The intersection of any one of these lines which express the condition for directivity with the line of zero-coupling slope constitutes a possible "design" configuration, defined here on the basis of both a flat coupling characteristic and good directivity.

Since a coupling formula is not available for the magnitude of coupling, the coupling length for a particular "design" configuration obtained graphically from Fig. 4 must be determined by measurement. The procedure used is to measure the coupling of a single hole in the configuration selected. Then the coupling for any number ($n$) of these holes in terms of the voltage coupling of one hole is approximately [4]:

$$C = \sin nc. \quad (9)$$

For full coupling, $C$ is unity, therefore the number of holes required for full coupling is

$$N = \pi/2c. \quad (10)$$

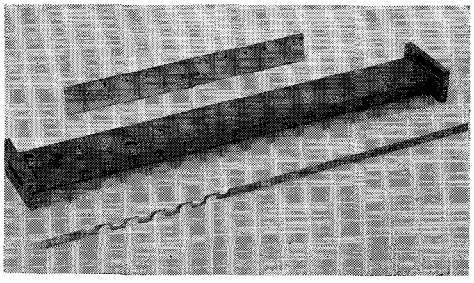

(a) Directional coupler.

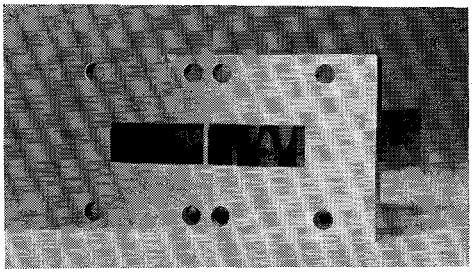

(b) Coupler-type bend.

Fig. 5. Normal-incidence test fixture.

## V. Illustrative Example

The selection of a configuration for the illustrative example was based on the requirement of keeping the coupling length small. It was previously mentioned that there are any number of "design" configurations. The configuration for minimum length requires the largest hole diameter and this configuration corresponds to the point on the graph in Fig. 4 labeled "design configuration with strongest coupling." From this point, a value of wall separation ($a=0.665\lambda$), and a nominal value of hole diameter ($d=0.415\lambda$) were obtained. The angle $\alpha$ corresponding to this configuration is 30°. The wall thickness was chosen to be $0.034\lambda$ which was the minimum thought to be mechanically practical in this case. A thicker wall would have resulted in the loading of the antisymmetric mode and therefore would result in an increase of the length required for full coupling.

In order to check the validity of the theory, the coupling of several holes having diameters near the nominal was measured. From these measurements, the hole having the flattest coupling characteristic with frequency was found to be $d=0.428\lambda$, which is very close to that predicted on the basis of theory. The voltage coupling coefficient, $c$, for this hole at midband was measured to be $c=0.15$. The next step was to build a directional coupler to simulate normal incidence. The number of holes for complete coupling was estimated to be 10 holes on the basis of (10). In order to ensure sufficient separation between adjacent holes for mechanical strength, it was found necessary to enlarge the triangular grid on which the holes are located; the resulting deviation in spacing from the optimum for this "design configuration" was not expected to result in a significant degradation of directivity. On the basis of measurements it was found neces-

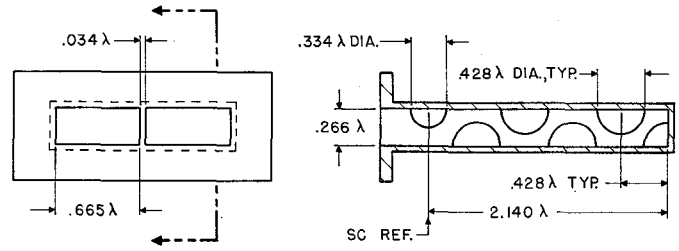


(a) Dimensions of the bend.

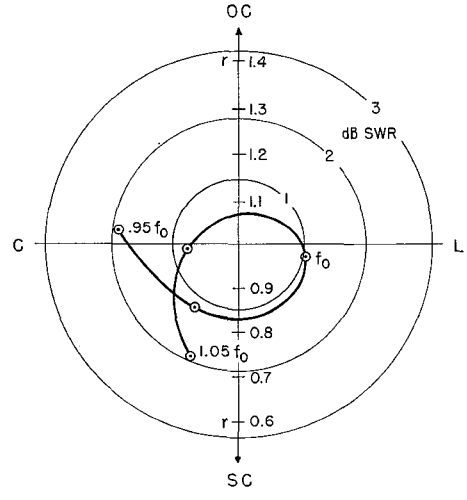


(b) Reflection of the bend.

Fig. 6. Bend design at normal incidence.

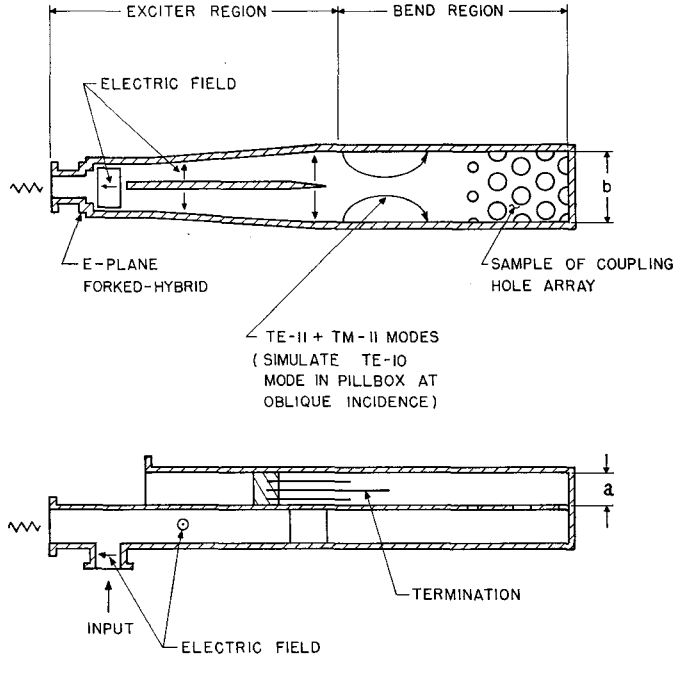


Fig. 7. Test fixture for simulation of bend at oblique incidence.

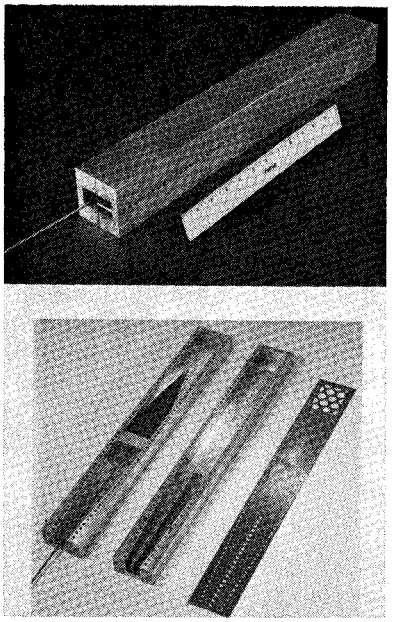

Fig. 8. Oblique-incidence coupler-type bend.

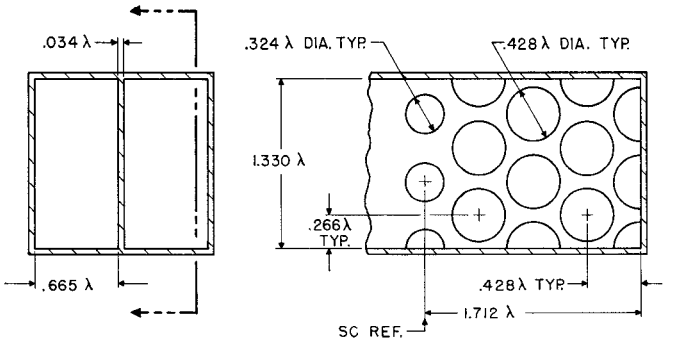


(a) Dimensions of bend.

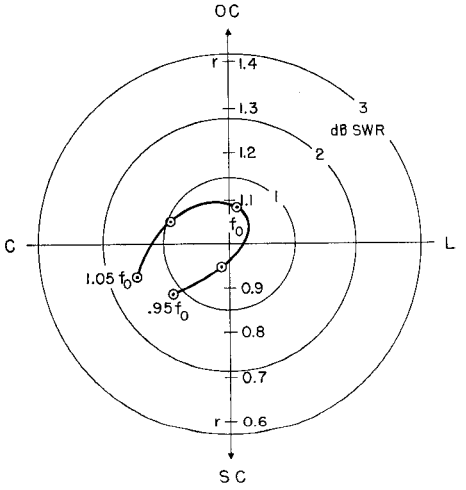


(b) Reflection of bend.

Fig. 9. Bend design for an incident angle of 37°.

sary to vary the diameter of the first and last holes of the coupler as trimmers in order to obtain complete coupling.

Shown in Fig. 5 are test fixtures for both the directional coupler and the coupler-type bend. The dimensions and performance of the bend at normal incidence are shown in Fig 6. The reflection of the bend was measured to be less than 2 dB SWR over a ten percent frequency band. This is in agreement with predictions based on the measured performance of the coupler.

The effective number of holes in the bend at oblique incidence was found by multiplying the effective number of holes in the bend at normal incidence by the normalized coupling length ($L/L_0$), plotted in Fig. 3. This effective number of holes is defined as the number of full-size holes plus an additional term representing the coupling effect of the leading hole whose diameter is smaller. This term is approximately the cube of the ratio of the leading-hole diameter to full-size hole diameter.

In order to verify the design at oblique incidence, a special type of fixture was devised which simulates the incident waves in the pillbox; it is illustrated by cross-sectional views in Fig. 7. The fixture is fed by an *E*-plane forked hybrid which excites the TE-11 and TM-11 modes in the correct relative amplitudes for proper simulation of the fields in the pillbox. The "*b*" dimension in the fixture determines the angle of incidence being simulated; it must also be of such a value so as to properly image the holes in the array. Thus, there are only a discrete number of simulations possible, each one corresponding to a different incident angle [7]. The reflection of the bend was determined by measuring the standing-wave ratio in the difference arm of the hybrid. Figure 8 is a photograph of the fixture; it is shown without the forked hybrid. The dimensions of the coupling region and the measured reflection for an angle of incidence of 37° are shown in Fig. 9.

In order to verify the performance of the entire bend, a model of the pillbox was constructed. Measurements of the performance of the pillbox included patterns, reflection, and cross-polarization response. The total reflection into the feed was less than 1 dB SWR over a ten percent frequency band. This included the reflection of the aperture, feed-horn, and support posts as well as the reflection caused by the bend. It should be noted that only a portion of the reflection caused by the bend is received by the horn. This is because the reflection from the bend travels back toward the feed as a plane wave which occupies the entire pillbox layer. Therefore, the feed intercepts only a small portion of this reflected wave. The reflection estimated to be directly caused by the bend is 0.2 dB SWR. The remainder reflects from the back wall enclosing the lower layer, and radiates from the aperture in a defocused pattern.

The cross-polarized response was also measured. This was accomplished by measuring the cross-polarized radiation patterns of the antenna. From these patterns, the cross-polarized signal was found to be −22 dB below the normal polarized signal.

## VI. Conclusions

The *H*-plane coupler-type bend has been found to yield a significant improvement in the performance of double-layer pillboxes as compared to previous designs in terms of reflection and cross-polarization. It has been found that the theory developed in designing the bend is sufficient to enable calculation of the principal dimensions of the bend, requiring only minor adjustments based on measurements for a complete design. The existence of an optimum hole diameter for achieving the shortest coupling length, consistent with a flat frequency characteristic and good directivity, has been hypothesized and verified. Performance of the coupler-type bend has been demonstrated in a wide-angle pillbox model.

## VII. Acknowledgment

The work described was performed under the direction of T. W. Madigan of Bell Telephone Laboratories. The coupler-type bend was based on an invention of D. S. Lerner, then at Wheeler Laboratories. The authors wish to thank H. A. Wheeler and N. A. Spencer for their helpful suggestions and guidance. The model of the pillbox used for the measurements was supplied by Bell Telephone Laboratories, who also provided programming assistance and computer time for the calculation of coupler hole patterns.

## VIII. References

[1] S. Silver, *Microwave Antenna Theory and Design*. New York: McGraw-Hill, 1949, pp. 460–464. (Single-layer pillbox.)
[2] H. Jasik, *Antenna Engineering Handbook*. New York: McGraw-Hill, 1961, pp. 12–19. (Single- and double-layer pillboxes.)
[3] D. S. Lerner, "Coupler-type bend," U. S. Patent 3 255 456, June 7, 1966.
[4] S. E. Miller, "Coupled wave theory and waveguide applications," *Bell Sys. Tech. J.*, vol. 33, p. 661, May 1954. (Comprehensive treatment of coupling between transmission lines.)
[5] K. Tomiyasu and S. B. Cohn, "The transvar directional coupler," *Proc. IRE*, vol. 41, pp. 922–926, July 1953. (Modal analysis of coupling.)
[6] S. B. Cohn, "Microwave coupling by large apertures," *Proc. IRE*, vol. 40, pp. 696–699, June 1952. (Variation of coupling with frequency for large holes.)
[7] P. W. Hannan and M. A. Balfour, "Simulation of a phased-array antenna in waveguide," *IEEE Trans. Antennas and Propagation*, vol. AP-13, pp. 342–353, May 1965. (Discussion of discrete simulation of periodic structures.)
[8] V. Mazzola, "A wideband tight directional coupler," Polytechnic Institute of Brooklyn, Brooklyn, N. Y., MSEE Rept., 1964.

# A Parallel-Plate Waveguide Approach to Microminiaturized, Planar Transmission Lines for Integrated Circuits

HENRY GUCKEL, MEMBER, IEEE, PIERCE A. BRENNAN, AND ISTVÁN PALÓCZ, SENIOR MEMBER, IEEE

***Abstract*—The parallel-plate waveguide with a two-layer loading medium, a conducting semiconductor substrate, and a relatively thin dielectric layer approximates the interconnections in many integrated systems if the fringing fields are ignored. The fundamental mode of this structure is an *E* mode which is a surface wave. Its propagation behavior is analyzed in this paper and the equations are evaluated by highly accurate numerical methods.**

**The semiconducting substrate is characterized by its dielectric constant and conductivity. A critical conductivity $\sigma_{min}$ exists and is related to the cross sectional and material parameters. If the substrate conductivity is given by $\sigma_{min}$ then the attenuation constant of the line is a minimum. The same value of conductivity yields minimum phase distortion at maximum bandwidth. If the conductivity is larger than $\sigma_{min}$ the substrate acts as a poor conductor with associated skin effect; if it is smaller, lossy dielectric behavior results.**

**Analysis shows that it is appropriate to subdivide the frequency range into three intervals. The lowest-frequency interval is characterized by propagation which resembles diffusion. This is caused by the loss in the dielectric layer. The next frequency range extends to some upper frequency which is determined by substrate conductivity and the cross-sectional dimensions. In this interval, the phase velocity of the fundamental mode is controlled by the ratio of dielectric to semiconductor thickness, which, if typical interconnections are considered, implies a very low velocity. This property indicates that the structure can serve as a delay line. Further increases in frequency result in higher phase velocities. Skin effect and dielectric loss behavior describe the propagation in this third interval.**

Manuscript received May 23, 1966; revised December 16, 1966.

H. Guckel is with the IBM Watson Research Center, Yorktown Heights, N. Y. He is now on leave of absence to the Dept. of Elec. Engrg. and Computer Components Lab., Washington University, St. Louis, Mo.

P. A. Brennan is with the IBM Watson Research Center, Yorktown Heights, N. Y.

I. Palócz is with the Dept. of Elec. Engrg., New York University, Bronx, N. Y. He was formerly with the IBM Watson Research Center, Yorktown Heights, N. Y.